Optimization on Manifolds for Models using Second Order Differences

Ronny Bergmann*
Technische Universität Chemnitz

Kolloquium über Angewandte Mathematik,
Institut für Numerische und Angewandte Mathematik,
Georg-August-Universität Göttingen,

May 28, 2019.

*joint with with M. Bačák, P.-Y. Gousenbourger, F. Laus, J. Persch, G. Steidl, A. Weinmann

Contents

1. Introduction

Manifold-Valued Images

New data acquisition modalities lead to non-Euclidean range

- Interferometric synthetic aperture radar (InSAR)
- Surface normals, GPS data, wind, flow,...
- Diffusion tensors in magnetic resonance imaging (DT-MRI), covariance matrices
- Electron backscattered diffraction (EBSD)

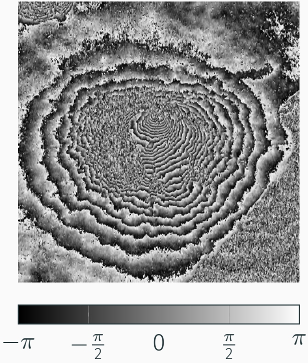

InSAR-Data of Mt. Vesuvius
[Rocca, Prati, Guarnieri, 1997]

phase-valued data, $\mathcal{M} = \mathbb{S}^1$

Manifold-Valued Images

New data acquisition modalities lead to non-Euclidean range

- Interferometric synthetic aperture radar (InSAR)
- Surface normals, GPS data, wind, flow,...
- Diffusion tensors in magnetic resonance imaging (DT-MRI), covariance matrices
- Electron backscattered diffraction (EBSD)

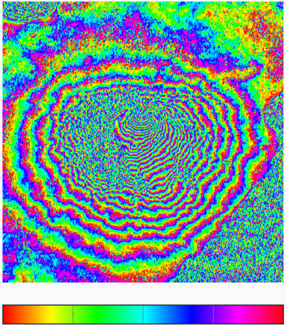

InSAR-Data of Mt. Vesuvius

[Rocca, Prati, Guarnieri, 1997]

phase-valued data, $\mathcal{M} = \mathbb{S}^1$

Manifold-Valued Images

New data acquisition modalities lead to non-Euclidean range

- Interferometric synthetic aperture radar (InSAR)
- Surface normals, GPS data, wind, flow,...
- Diffusion tensors in magnetic resonance imaging (DT-MRI), covariance matrices
- Electron backscattered diffraction (EBSD)

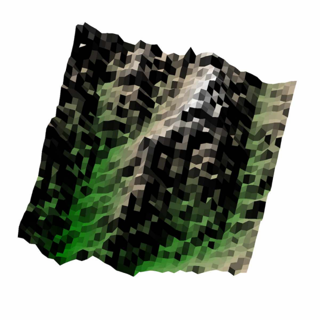

National elevation dataset
[Gesch et al., 2009]

directional data, $\mathcal{M} = \mathbb{S}^2$

Manifold-Valued Images

New data acquisition modalities lead to non-Euclidean range

- Interferometric synthetic aperture radar (InSAR)
- Surface normals, GPS data, wind, flow,...
- Diffusion tensors in magnetic resonance imaging (DT-MRI), covariance matrices
- Electron backscattered diffraction (EBSD)

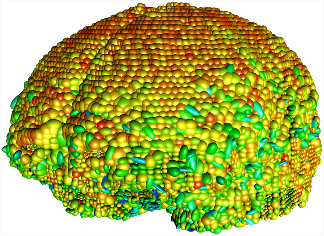

diffusion tensors in human brain
from the Camino dataset
http://cmic.cs.ucl.ac.uk/camino

sym. pos. def. matrices, $\mathcal{M} = \mathrm{SPD}(3)$

Manifold-Valued Images

New data acquisition modalities lead to non-Euclidean range

- Interferometric synthetic aperture radar (InSAR)
- Surface normals, GPS data, wind, flow,...
- Diffusion tensors in magnetic resonance imaging (DT-MRI), covariance matrices
- Electron backscattered diffraction (EBSD)

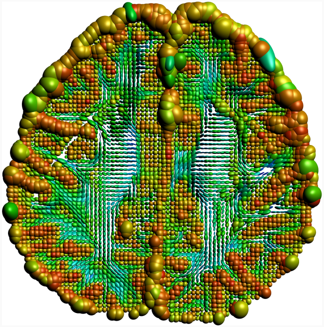

horizontal slice # 28
from the Camino dataset
http://cmic.cs.ucl.ac.uk/camino

sym. pos. def. matrices, $\mathcal{M} = \mathrm{SPD}(3)$

Manifold-Valued Images

New data acquisition modalities lead to non-Euclidean range

- Interferometric synthetic aperture radar (InSAR)
- Surface normals, GPS data, wind, flow,...
- Diffusion tensors in magnetic resonance imaging (DT-MRI), covariance matrices
- Electron backscattered diffraction (EBSD)

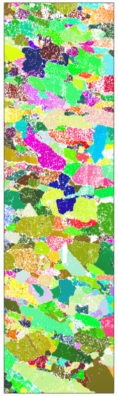

EBSD example from the MTEX toolbox
[Bachmann, Hielscher, since 2005]

Rotations (mod. symmetry), $\mathcal{M} = \mathrm{SO}(3)(/\mathcal{S})$.

Manifold-Valued Images

New data acquisition modalities lead to non-Euclidean range

- Interferometric synthetic aperture radar (InSAR)
- Surface normals, GPS data, wind, flow,…
- Diffusion tensors in magnetic resonance imaging (DT-MRI), covariance matrices
- Electron backscattered diffraction (EBSD)

Common properties

- Range of values is a Riemannian manifold
- Tasks from "classical" image processing, e.g.
  - denoising
  - inpainting
  - interpolation
  - labeling
  - deblurring

A d-dimensional Riemannian Manifold $\mathcal{M}$

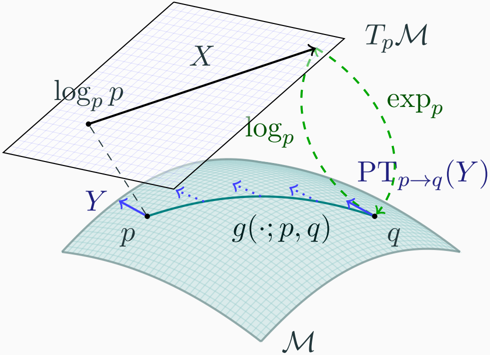

A d-dimensional Riemannian manifold can be informally defined as a set $\mathcal{M}$ covered with a 'suitable' collection of charts, that identify subsets of $\mathcal{M}$ with open subsets of $\mathbb{R}^d$ and a continuously varying inner product on the tangential spaces.

[Absil, Mahony, Sepulchre, 2008]

A d-dimensional Riemannian Manifold $\mathcal{M}$

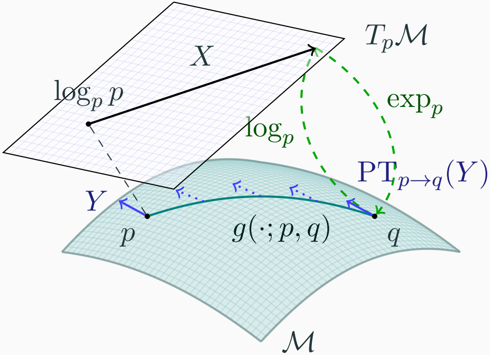

Geodesic $g(\cdot;p,q)$ shortest path (on $\mathcal{M}$) between $p, q \in \mathcal{M}$
Tangent space $\mathrm{T}_p\mathcal{M}$ at p, with inner product $(\cdot,\cdot)_p$
Logarithmic map $\log_p q = \dot{g}(0;p,q)$ "speed towards q"
Exponential map $\exp_p X = g(1)$, where $g(0) = p$, $\dot{g}(0) = X$
Parallel transport $\mathrm{PT}_{p\to q}(Y)$ of $Y \in \mathrm{T}_p\mathcal{M}$ along $g(\cdot;p,q)$

Variational Methods on Manifolds

Variational methods model a trade-off between staying close to the data and minimizing a certain property

$$\mathcal{E}(p) = D(p; f) + \alpha R(p), \quad p \in \mathcal{M}$$

- $\alpha > 0$ is a weight
- $\mathcal{M}$ is a Riemannian manifold
- given (input) data $f \in \mathcal{M}$
- data or similarity term $D(p; f)$
- regularizer / prior $R(p)$

Optimization on Manifolds

Let $\mathcal{M}$ and $\mathcal{N}$ be Riemannian Manifolds and $\mathcal{E}\colon \mathcal{N} \to \mathbb{R}$.

Consider the optimization problem

$$\operatorname*{arg\,min}_{p\in\mathcal{N}} \mathcal{E}(p)$$

where $\mathcal{E}$ is

- (maybe) non-smooth
- (locally) convex
- high-dimensional,
  - a manifold valued signal, $\mathcal{N} = \mathcal{M}^d$
  - a manifold-valued image, $\mathcal{N} = \mathcal{M}^{d_1\times d_2}$
- decomposable $\mathcal{E} = F + G$ in two (or even more) summands

A Signal of Cyclic Data

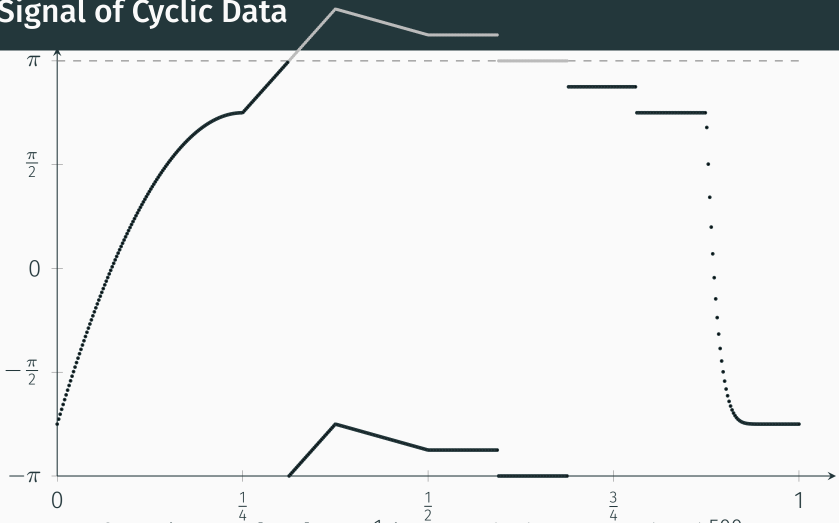

- A function $f\colon [0,1] \to \mathbb{S}^1$ is sampled $\Rightarrow f_\mathrm{o} = (f_{\mathrm{o},i})_{i=1}^{500}$
- Data f stems from the gray plot via modulo
- Jumps $> \pi$ at $\frac{5}{16}$ and $\frac{11}{16}$ just from choice of representation

A Signal of Cyclic Data

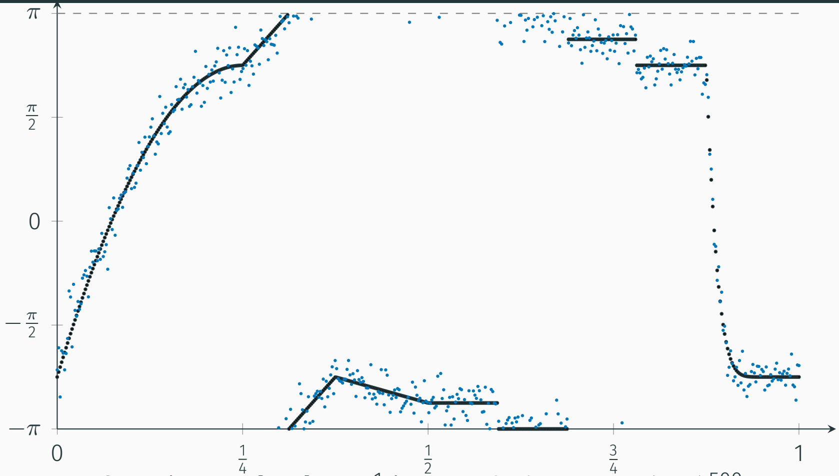

- A function $f\colon [0,1] \to \mathbb{S}^1$ is sampled $\Rightarrow f_o = (f_{o,i})_{i=1}^{500}$
- Noise: wrapped Gaussian, $\sigma = 0.2$
- noisy $f_n = (f_o + \eta)_{2\pi}$

A Signal of Cyclic Data

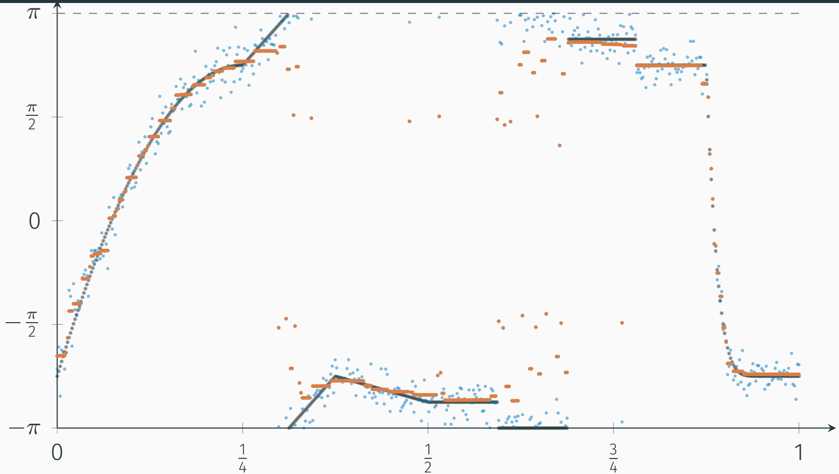

- Comparison of f_{o} & f_{n} width f_{R}
- Denoised with CPPA and realvalued TV_1, ($\alpha = \frac{3}{4}$, $\beta = 0$)
- Artefacts at the “jumps that are none“ from representation

A Signal of Cyclic Data

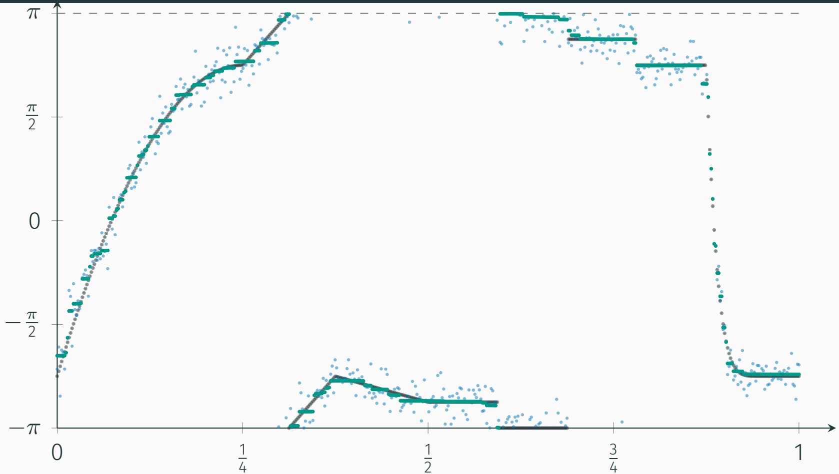

- Comparison of f_o & f_n width f_1
- Denoised with CPPA and TV_1 ($\alpha = \frac{3}{4}$, $\beta = 0$)
- but: stair caising

A Signal of Cyclic Data

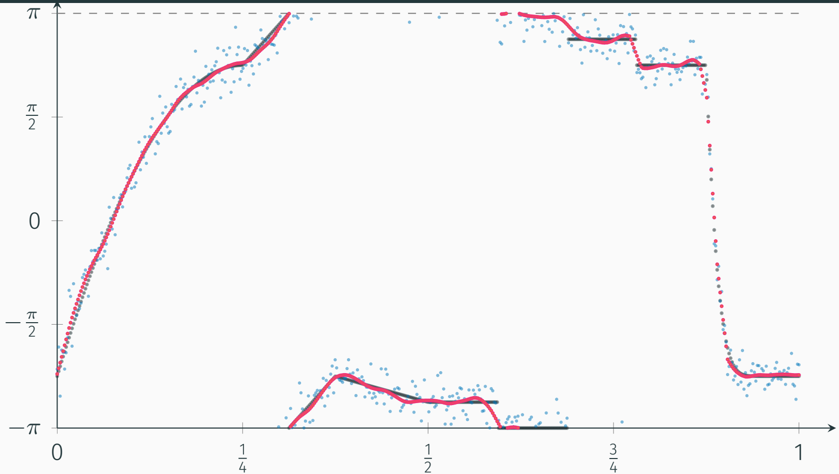

- Comparison of f_o & f_n width f_2
- Denoised with CPPA and TV_2 $(\alpha = 0, \beta = \frac{3}{2})$
- but: problems in constant areas

A Signal of Cyclic Data

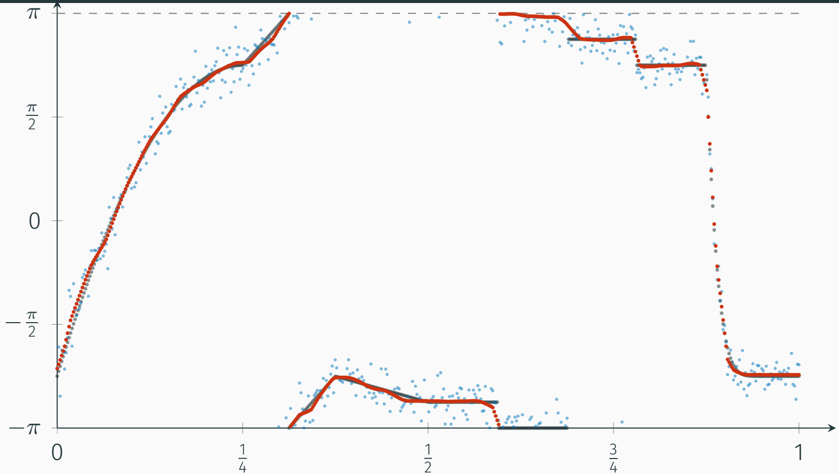

- Comparison of f_o & f_n width f_3
- Denoised with CPPA and TV_1 & TV_2 $(\alpha = \frac{1}{4}, \beta = \frac{3}{4})$
- combined: smallest mean squared error.

2. Second Order Differences

First and Second Order Differences

On $\mathbb{R}^n$

- line $\gamma(t) = x + t(y-x)$
- distance $\|x-y\|_2$
- first order model

[Rudin, Osher, Fatemi, 1992]

$$\sum_{i\in\mathcal{V}}\|f_i-u_i\|_2^2+\alpha\sum_{i\in\mathcal{G}\setminus\{N\}}\|u_i-u_{i+1}\|_2$$

Riemannian manifold $\mathcal{M}$

- geodesic path $g(t;p,q)$
- geodesic distance $d\colon \mathcal{M}\times\mathcal{M}\to\mathbb{R}$
- first order model

[Strekalovskiy, Cremers, 2011; Lellmann et al., 2013, Weinmann, Demaret, Storath, 2014]

$$\sum_{i\in\mathcal{V}} d(f_i,u_i)^2 + \alpha \sum_{i\in\mathcal{G}\setminus\{N\}} d(u_i,u_{i+1})$$

First and Second Order Differences

On $\mathbb{R}^n$

- line $\gamma(t) = x + t(y-x)$
- distance $\|x-y\|_2$
- first order model [Rudin, Osher, Fatemi, 1992]

$$\sum_{i\in\mathcal{V}}\|f_i-u_i\|_2^2+\alpha\sum_{i\in\mathcal{G}\setminus\{N\}}\|u_i-u_{i+1}\|_2$$

- second oder difference

$$\|x-2y+z\|_2$$

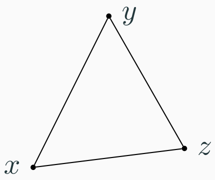

Riemannian manifold $\mathcal{M}$

- geodesic path $g(t;p,q)$
- geodesic distance $d\colon \mathcal{M}\times\mathcal{M}\to\mathbb{R}$
- first order model [Strekalovskiy, Cremers, 2011; Lellmann et al., 2013, Weinmann, Demaret, Storath, 2014]

$$\sum_{i\in\mathcal{V}} d(f_i,u_i)^2 + \alpha \sum_{i\in\mathcal{G}\setminus\{N\}} d(u_i,u_{i+1})$$

- How to model that on $\mathcal{M}$?

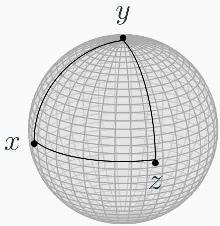

$\mathcal{M} = \mathbb{S}^2$

First and Second Order Differences

On $\mathbb{R}^n$

- line $\gamma(t) = x + t(y-x)$
- distance $\|x-y\|_2$
- first order model

[Rudin, Osher, Fatemi, 1992]

$$\sum_{i\in\mathcal{V}}\|f_i-u_i\|_2^2+\alpha\sum_{i\in\mathcal{G}\setminus\{N\}}\|u_i-u_{i+1}\|_2$$

- second oder difference

$$2\|\tfrac{1}{2}(x+z)-y\|_2$$

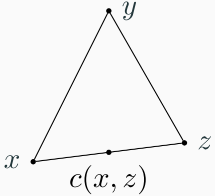

Riemannian manifold $\mathcal{M}$

- geodesic path $g(t;p,q)$
- geodesic distance $d\colon \mathcal{M}\times\mathcal{M}\to\mathbb{R}$
- first order model

[Strekalovskiy, Cremers, 2011; Lellmann et al., 2013, Weinmann, Demaret, Storath, 2014]

$$\sum_{i\in\mathcal{V}} d(f_i,u_i)^2 + \alpha \sum_{i\in\mathcal{G}\setminus\{N\}} d(u_i,u_{i+1})$$

- idea: mid point formulation

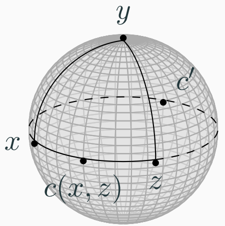

$\mathcal{M} = \mathbb{S}^2$

First and Second Order Differences

On $\mathbb{R}^n$

- line $\gamma(t) = x + t(y - x)$
- distance $\|x - y\|_2$
- first order model

[Rudin, Osher, Fatemi, 1992]

$$\sum_{i\in\mathcal{V}}\|f_i-u_i\|_2^2+\alpha\sum_{i\in\mathcal{G}\setminus\{N\}}\|u_i-u_{i+1}\|_2$$

- second oder difference

$$2\|c(x,z) - y\|_2$$

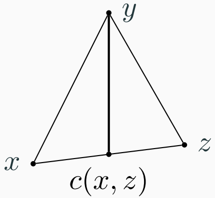

Riemannian manifold $\mathcal{M}$

- geodesic path $g(t;p,q)$
- geodesic distance $d\colon \mathcal{M}\times\mathcal{M}\to\mathbb{R}$
- first order model

[Strekalovskiy, Cremers, 2011; Lellmann et al., 2013, Weinmann, Demaret, Storath, 2014]

$$\sum_{i\in\mathcal{V}} d(f_i,u_i)^2 + \alpha \sum_{i\in\mathcal{G}\setminus\{N\}} d(u_i,u_{i+1})$$

- idea: mid point formulation

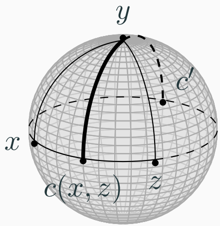

$\mathcal{M} = \mathbb{S}^2$

Absolute Second Order Difference

We denote the set of mid points between $x, z \in \mathcal{M}$ as

$\mathcal{C}_{x,z} := \{c \in \mathcal{M} : c = g(\frac{1}{2}; x, z)$ for any geodesic $g(\cdot; x, z) \colon [0, 1] \to \mathcal{M}\}$

and define the Absolute Second Order Difference

[Bergmann, Laus, et al., 2014; Bačák et al., 2016]

$$d_2(x, y, z) := \min_{c \in \mathcal{C}_{x,z}} d(c, y), \qquad x, y, z \in \mathcal{M}.$$

For Optimization we need the differential and gradient of d_2 with respect to all its three arguments. For example for the first argument we have a chain rule of the distance and $g(\frac{1}{2}; \cdot, z)$

Differential and Gradient

The differential $D_p f = Df\colon T\mathcal{M} \to \mathbb{R}$ of a real-valued function $f\colon \mathcal{M} \to \mathbb{R}$ is the push-forward of f.

For a composition $F(p) = (g \circ h)(p) = g(h(p))$ of two functions $g, h\colon \mathcal{M} \to \mathcal{M}$ the chain rule reads

$$D_p F[X] = D_{h(p)} g\bigl[D_p h[X]\bigr],$$

where $D_p h[X] \in T_{h(p)}\mathcal{M}$ and $D_p F[X] \in T_{F(p)}\mathcal{M}$.

The gradient $\nabla f\colon \mathcal{M} \to T\mathcal{M}$ is the tangent vector fulfilling

$$(\nabla_{\mathcal{M}} f(p), Y)_p = Df(p)[Y] \text{ for all } Y \in T_p\mathcal{M},$$

i.e. $\nabla f(p) \in T_p\mathcal{M}$ is a tangent vector at p.

The Differential of a Geodesic w.r.t. its Start Point

The geodesic variation

$$\Gamma_{g,X}(s,t) \coloneqq \exp_{g_{p,X}(s)}(tY(s)), \qquad s \in (-\varepsilon,\varepsilon),\ t \in [0,1], \varepsilon > 0.$$

is used to define the Jacobi field $J_{g,X}(t) = \frac{\partial}{\partial s}\Gamma_{g,X}(s,t)|_{s=0}$.

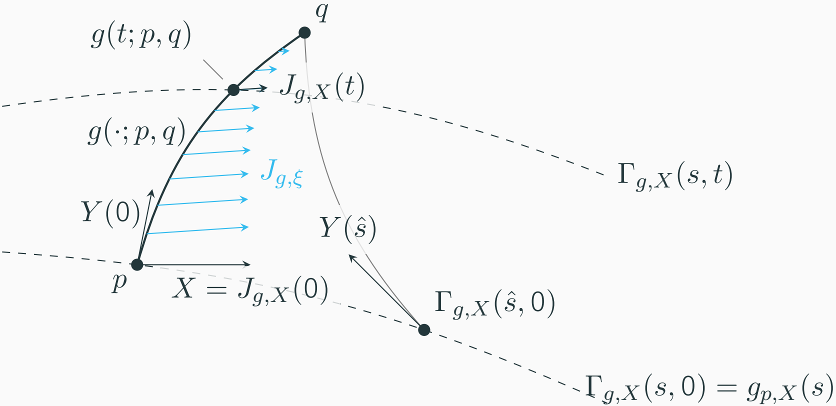

Then the differential reads $D_p g(t;\cdot,q)[X] = J_{g,X}(t)$.

Implementing Jacobi Fields on Symmetric Spaces

A manifold is symmetric if for every geodesic g and every $p \in \mathcal{M}$ the mapping $g(t) \mapsto g(-t)$ is an isometry at least locally around $p = g(0)$.

Then the system of ODEs characterizing the Jacobi field

$$\frac{D^2}{\mathrm{d}t^2} J_{g,X} + R(J_{g,X}, \dot{g})\dot{g} = 0, \qquad J_{g,X}(0) = X,\ J_{g,X}(1) = 0$$

- has constant coefficients
- one can diagonalize the curvature tensor R,
- let κ_ℓ denote its eigenvalues
- let $\{X_1, \ldots, X_d\} \subseteq T_p\mathcal{M}$ be an ONB to these eigenvalues with $X_1 = \log_p q$.
- parallel transport $\Xi_j(t) = \mathrm{PT}_{p \to g(t;p,q)} X_j$, $j = 1, \ldots, d$

Decompose $X = \sum_{i=1}^{d} \eta_\ell X_\ell$. Then

$$D_p g(t; p, q)[X] = J_{g,X}(t) = \sum_{\ell=1}^{d} \eta_\ell J_{g,X_\ell}(t),$$

with

$$J_{g,X_\ell}(t) = \begin{cases} \frac{\sinh\left(d_g(1-t)\sqrt{-\kappa_\ell}\right)}{\sinh(d_g\sqrt{-\kappa_\ell})}\Xi_\ell(t) & \text{if } \kappa_\ell < 0, \\ \frac{\sin\left(d_g(1-t)\sqrt{\kappa_\ell}\right)}{\sin(\sqrt{\kappa_\ell} d_g)}\Xi_\ell(t) & \text{if } \kappa_\ell > 0, \\ (1-t)\Xi_\ell(t) & \text{if } \kappa_\ell = 0, \end{cases}$$

where $d_g = d(p, q)$ is the length of the geodesic.

Implementing the Gradient Using Adjoint Jacobi Fields.

The adjoint Jacobi fields

$$J^*_{g,\cdot}(t)\colon T_{g(t;p,q)}\mathcal{M} \to T_p\mathcal{M}$$

are characterized by

$$(J_{g,X}(t), Y)_{g(t)} = (X, J^*_{g,Y}(t))_p, \text{ for all } X \in T_p\mathcal{M}, Y \in T_{g(t;p,q)}\mathcal{M}.$$

- computed using the same ODEs

$\Rightarrow$ calculate gradient of $f(x) = d\big(y, c\big), c = g(\frac{1}{2}; x, z)$, as

$$\nabla f(x) = J^*_{g,Y}(\tfrac{1}{2}), \quad g = g(\cdot; x, z),\ Y = -\frac{\log_c y}{\|\log_c y\|_c}$$

- the gradient of iterated evaluations of geodesics
  $\Rightarrow$ (sum of) composition of (adjoint) Jacobi fields

3. Second Order Total Variation

A Second Order TV-type Model on Manifolds

For $\mathcal{M}$-valued signals f we can hence define

$$\mathcal{E}(u) \coloneqq \sum_{i \in \mathcal{V}} d(f_i, u_i)^2 + \alpha \sum_{i \in \mathcal{G} \setminus \{N\}} d(u_i, u_{i+1}) + \beta \sum_{i \in \mathcal{G} \setminus \{1,N\}} d_2(u_{i-1}, u_i, u_{i+1})$$

A Second Order TV-type Model on Manifolds

For $\mathcal{M}$-valued signals f we can hence define

$$\mathcal{E}(u) := \sum_{i\in\mathcal{V}} d(f_i,u_i)^2 + \alpha \sum_{i\in\mathcal{G}\setminus\{N\}} d(u_i,u_{i+1}) + \beta \sum_{i\in\mathcal{G}\setminus\{1,N\}} d_2(u_{i-1},u_i,u_{i+1})$$

For images additionally: use
$\|w-x+y-z\|_2 = 2\|\frac{1}{2}(w+y) - \frac{1}{2}(x+z)\|_2$ for
Absolute Second Order Mixed Difference

$$d_{1,1}(w,x,y,z) := \min_{c\in\mathcal{C}_{w,y},\tilde{c}\in\mathcal{C}_{x,z}} d(c,\tilde{c}), \qquad w,x,y,z\in\mathcal{M}.$$

Proximal Map

For $\varphi\colon \mathcal{M}^n \to (-\infty, +\infty]$ and $\lambda > 0$ we define the Proximal Map as [Moreau, 1965; Rockafellar, 1976; Ferreira, Oliveira, 2002]

$$\operatorname{prox}_{\lambda\varphi}(p) := \operatorname*{arg\,min}_{u\in\mathcal{M}^n} \frac{1}{2}\sum_{i=1}^{n} d(u_i, p_i)^2 + \lambda\varphi(u).$$

! For a Minimizer u^* of φ we have $\operatorname{prox}_{\lambda\varphi}(u^*) = u^*$.

- For $\varphi\colon \mathbb{R}^n \to \mathbb{R}$ proper, convex, lower semicontinuous:
  - the $\operatorname{proximal}$ map is unique.
  - PPA $x_k = \operatorname{prox}_{\lambda\varphi}(x_{k-1})$ converges to $\operatorname{arg\,min}\varphi$
- For $\varphi = \mathcal{E}$ not that useful

The Cyclic Proximal Point Algorithm

For $\varphi = \sum_{l=1}^{c} \varphi_l$ the

Cyclic Proximal Point-Algorithmus (CPPA) reads [Bertsekas, 2011; Bačák, 2014]

$$p^{(k+\frac{l+1}{c})} = \operatorname{prox}_{\lambda_k \varphi_l}(p^{(k+\frac{l}{c})}), \quad l = 0, \ldots, c-1,\ k = 0, 1, \ldots$$

On a Hadamard manifold $\mathcal{M}$:
convergence to a minimizer of φ if

- all φ_l proper, convex, lower semicontinuous
- $\{\lambda_k\}_{k\in\mathbb{N}} \in \ell_2(\mathbb{N})\setminus\ell_1(\mathbb{N})$.

Ansatz.

- efficient Proximal Maps for every summand of $\mathcal{E}(u)$.
- speed up by parallelization

Proximal Maps for Distance and TV summands

Let $g(\cdot; p, q)\colon [0,1] \to \mathcal{M}$ be a geodesic between $p, q \in \mathcal{M}$.

Theorem (Distance term) **[Ferreira, Oliveira, 2002]**
For $\varphi(p) = d^2(p, f)$ with fixed $f \in \mathcal{M}$ we have

$$\operatorname{prox}_{\lambda\varphi}(p) = g\Big(\frac{\lambda d(p,f)}{1+\lambda d(p,f)}; p, f\Big)$$

Theorem (First Order Difference Term) **[Weinmann, Demaret, Storath, 2014]**
For $\varphi(p, q) = d(p, q)$ we have

$$\operatorname{prox}_{\lambda\varphi}(p, q) = \big(g(t; p, q), g(1-t; p, q)\big)$$

with

$$t = \begin{cases} \frac{\lambda}{d(p,q)} & \text{if } \lambda < \frac{1}{2}d(p,q) \\ \frac{1}{2} & \text{else.} \end{cases}$$

Proximal Maps for the TV_2 Summands

To compute

$$\operatorname{prox}_{\lambda d_2}(p) = \operatorname*{arg\,min}_{u \in \mathcal{M}^3} \Bigl\{ \frac{1}{2} \sum_{i=1}^{3} d(u_i, p_i)^2 + \lambda d_2(u_1, u_2, u_3) \Bigr\}$$

We have

- a closed form solution for $\mathcal{M} = \mathbb{S}^1$ [Bergmann, Laus, et al., 2014]
- use a sub gradient descent (as inner problem) with

$$\nabla_{\mathcal{M}^3} d_2 = \bigl(\nabla_{\mathcal{M}} d_2(\cdot, p_2, p_3), \nabla_{\mathcal{M}} d_2(p_1, \cdot, p_3), \nabla_{\mathcal{M}} d_2(p_1, p_2, \cdot)\bigr)^{\mathrm{T}}.$$

where

- $\nabla_{\mathcal{M}} d_2(p_1, \cdot, p_3)(y) = -\frac{\log_y c(p_1, p_3)}{\lVert \log_{p_2} c(p_1, p_3) \rVert_{p_2}} \in T_y\mathcal{M}$
- $\nabla_{\mathcal{M}} d_2(\cdot, p_2, p_3)$ and analogously $\nabla_{\mathcal{M}} d_2(p_1, p_2, \cdot)$ using (adjoint) Jacobi fields and a chain rule [Bačák et al., 2016]

Bernoulli's Lemniscate on the sphere $\mathbb{S}^2$

$$\gamma(t) \coloneqq \frac{a\sqrt{2}}{\sin^2(t)+1}\bigl(\cos(t), \cos(t)\sin(t), 1\bigr)^{\mathrm{T}}, \quad t \in [0, 2\pi], a = \frac{\pi}{2\sqrt{2}}.$$

Generate a sphere-valued signal by

$$\gamma_S(t) = \exp_p(\gamma(t)), p = (0,0,1)^{\mathrm{T}}$$

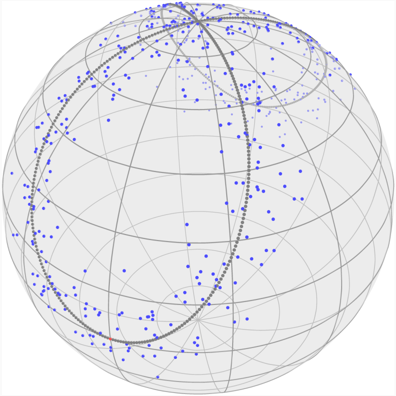

noisy lemniscate of Bernoulli on $\mathbb{S}^2$, Gaussian noise, $\sigma = \frac{\pi}{30}$, on $T_p\mathbb{S}^2$.

Bernoulli's Lemniscate on the sphere $\mathbb{S}^2$

$$\gamma(t) \coloneqq \frac{a\sqrt{2}}{\sin^2(t)+1}\big(\cos(t), \cos(t)\sin(t), 1\big)^{\mathrm{T}}, \quad t \in [0, 2\pi], a = \frac{\pi}{2\sqrt{2}}.$$

Generate a sphere-valued signal by

$$\gamma_S(t) = \exp_p(\gamma(t)), p = (0, 0, 1)^{\mathrm{T}}$$

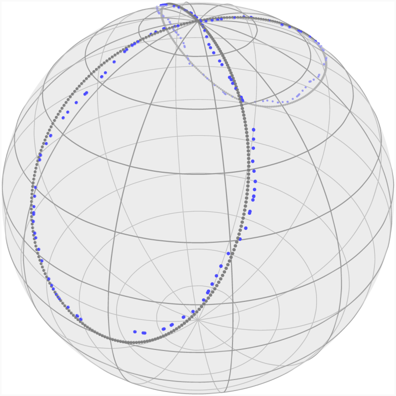

reconstruction with TV_1, $\alpha = 0.21$, MAE $= 4.08 \times 10^{-2}$.

Bernoulli's Lemniscate on the sphere $\mathbb{S}^2$

$$\gamma(t) \coloneqq \frac{a\sqrt{2}}{\sin^2(t)+1}\bigl(\cos(t), \cos(t)\sin(t), 1\bigr)^{\mathrm{T}}, \quad t \in [0, 2\pi], a = \frac{\pi}{2\sqrt{2}}.$$

Generate a sphere-valued signal by

$$\gamma_S(t) = \exp_p(\gamma(t)), p = (0,0,1)^{\mathrm{T}}$$

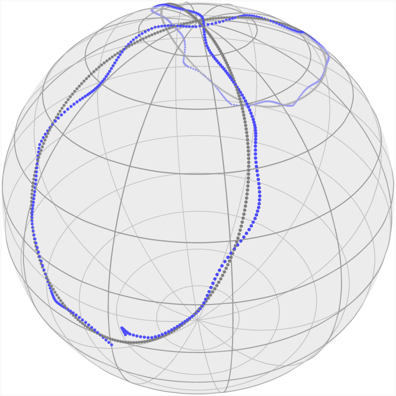

reconstruction with TV_2, $\alpha = 0$, $\beta = 10$, $\mathrm{MAE} = 3.66 \times 10^{-2}$.

$$\gamma(t) \coloneqq \frac{a\sqrt{2}}{\sin^2(t)+1}\big(\cos(t), \cos(t)\sin(t), 1\big)^{\mathrm{T}}, \quad t \in [0, 2\pi], a = \frac{\pi}{2\sqrt{2}}.$$

Generate a sphere-valued signal by

$$\gamma_S(t) = \exp_p(\gamma(t)), p = (0,0,1)^{\mathrm{T}}$$

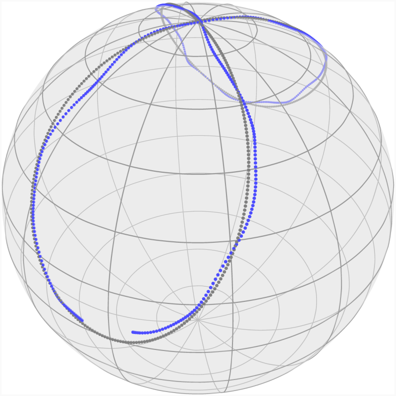

reconstruction with TV_1 & TV_2, $\alpha = 0.16$, $\beta = 12.4$, MAE $= 3.27 \times 10^{-2}$.

Inpainting of $\mathcal{P}(3)$-valued Images

Draw symmetric positive definite 3×3 matrices as ellipsoids

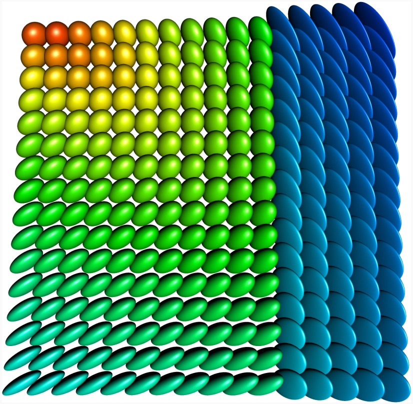

original data

Inpainting of $\mathcal{P}(3)$-valued Images

Draw symmetric positive definite 3×3 matrices as ellipsoids

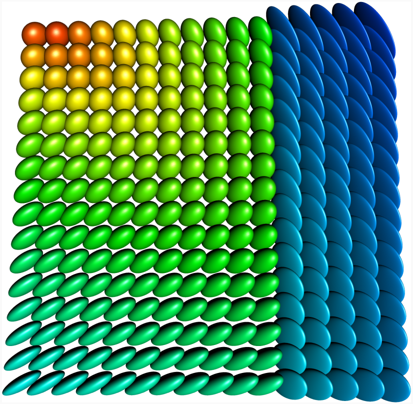

original data

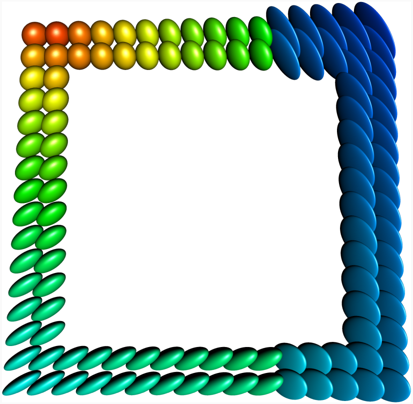

lost (a lot of) data

Inpainting of $\mathcal{P}(3)$-valued Images

Draw symmetric positive definite 3×3 matrices as ellipsoids

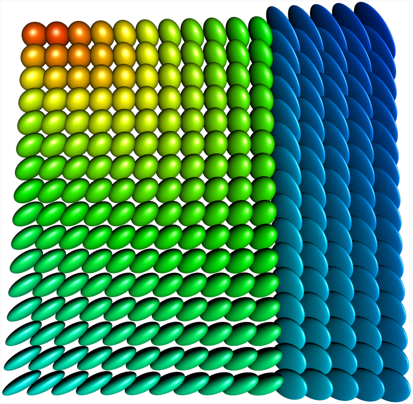

original data

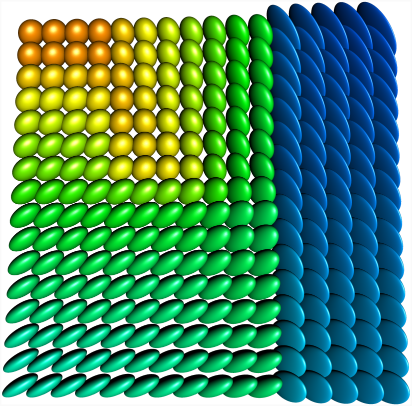

inpainted with $\alpha = \beta = 0.05$,

MAE $= 0.0929$

Inpainting of $\mathcal{P}(3)$-valued Images

Draw symmetric positive definite 3×3 matrices as ellipsoids

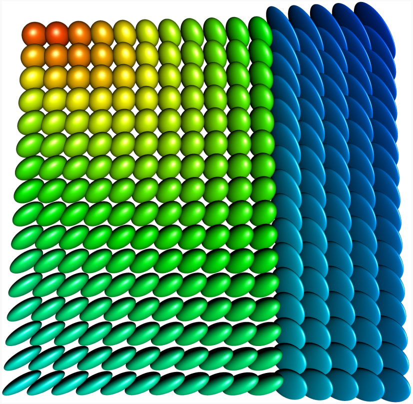

original data

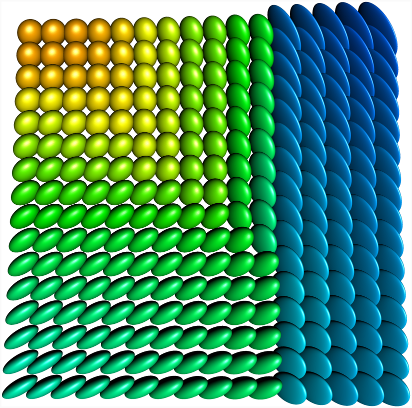

inpainted with $\alpha = 0.1$,

MAE $= 0.0712$

4. Acceleration of Bézier Curves

Data Fitting on Manifolds

Given data points $d_0, \ldots, d_n$ on a Riemannian manifold $\mathcal{M}$ and time points $t_i \in I$, find a "nice" curve $\gamma \colon I \to \mathcal{M}$, $\gamma \in \Gamma$, such that $\gamma(t_i) = d_i$ (interpolation) or $\gamma(t_i) \approx d_i$ (approximation).

Data Fitting on Manifolds

Given data points $d_0, \dots, d_n$ on a Riemannian manifold $\mathcal{M}$ and time points $t_i \in I$, find a "nice" curve $\gamma\colon I \to \mathcal{M}$, $\gamma \in \Gamma$, such that $\gamma(t_i) = d_i$ (interpolation) or $\gamma(t_i) \approx d_i$ (approximation).

- Γ set of geodesics & approximation: geodesic regression [Rentmeesters, 2011; Fletcher, 2013; Boumal, Absil, 2011]
- Γ Sobolev space of curves: Inifinite-dimensional problem [Samir et al., 2012]
- Γ composite Bézier curves; LSs in tangent spaces [Arnould et al., 2015; Gousenbourger, Massart, Absil, 2018]
- Discretized curve, $\Gamma = \mathcal{M}^N$, [Boumal, Absil, 2011]

Data Fitting on Manifolds

Given data points $d_0, \ldots, d_n$ on a Riemannian manifold $\mathcal{M}$ and time points $t_i \in I$, find a "nice" curve $\gamma\colon I \to \mathcal{M}$, $\gamma \in \Gamma$, such that $\gamma(t_i) = d_i$ (interpolation) or $\gamma(t_i) \approx d_i$ (approximation).

- Γ set of geodesics & approximation: geodesic regression [Rentmeesters, 2011; Fletcher, 2013; Boumal, Absil, 2011]
- Γ Sobolev space of curves: Inifinite-dimensional problem [Samir et al., 2012]
- Γ composite Bézier curves; LSs in tangent spaces [Arnould et al., 2015; Gousenbourger, Massart, Absil, 2018]
- Discretized curve, $\Gamma = \mathcal{M}^N$, [Boumal, Absil, 2011]

This talk.

"nice" means minimal (discretized) acceleration ("as straight as possible") for Γ the set of composite Bézier curves.

Closed form solution for $\mathcal{M} = \mathbb{R}^d$: Natural (cubic) splines.

(Euclidean) Bézier Curves

Definition [Bézier, 1962]

A Bézier curve β_K of degree $K \in \mathbb{N}_0$ is a function $\beta_K \colon [0,1] \to \mathbb{R}^d$ parametrized by control points $b_0, \ldots, b_K \in \mathbb{R}^d$ and defined by

$$\beta_K(t; b_0, \ldots, b_K) := \sum_{j=0}^{K} b_j B_{j,K}(t),$$

[Bernstein, 1912]

where $B_{j,K} = \binom{K}{j} t^j (1-t)^{K-j}$ are the Bernstein polynomials of degree K.

Evaluation via Casteljau's algorithm. [de Casteljau, 1959]

Illustration of de Casteljau's Algorithm

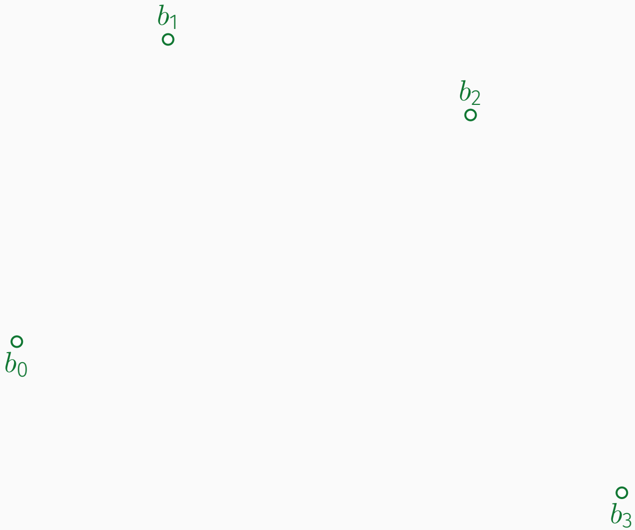

The set of control points b_0, b_1, b_2, b_3.

Illustration of de Casteljau's Algorithm

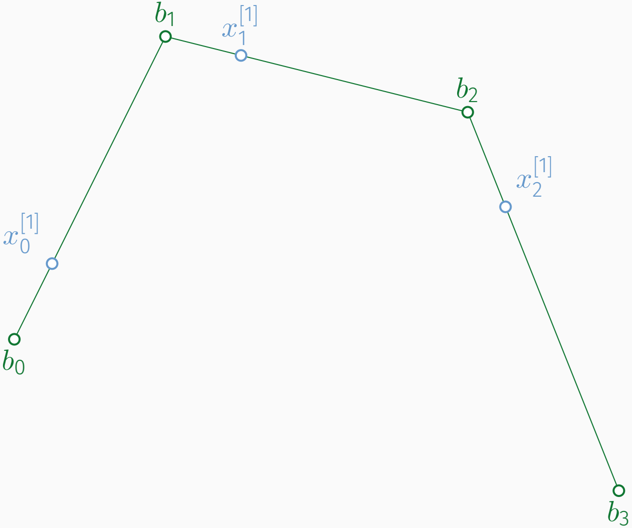

Evaluate line segments at $t = \frac{1}{4}$, obtain $x_0^{[1]}, x_1^{[1]}, x_2^{[1]}$.

Illustration of de Casteljau's Algorithm

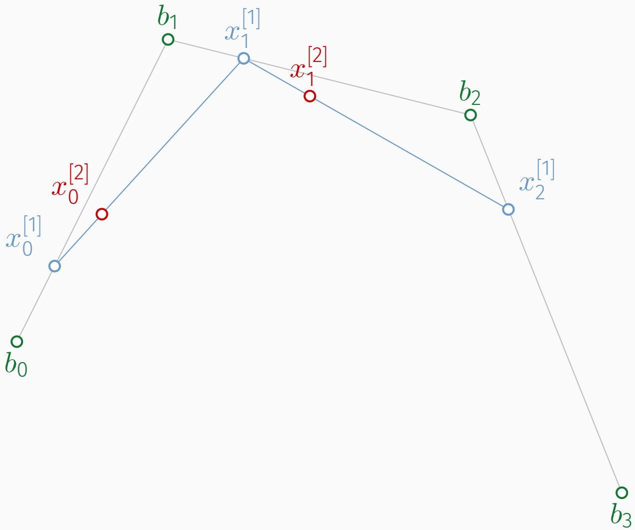

Repeat evaluation for new line segments to obtain $x_0^{[2]}, x_1^{[2]}$.

Illustration of de Casteljau's Algorithm

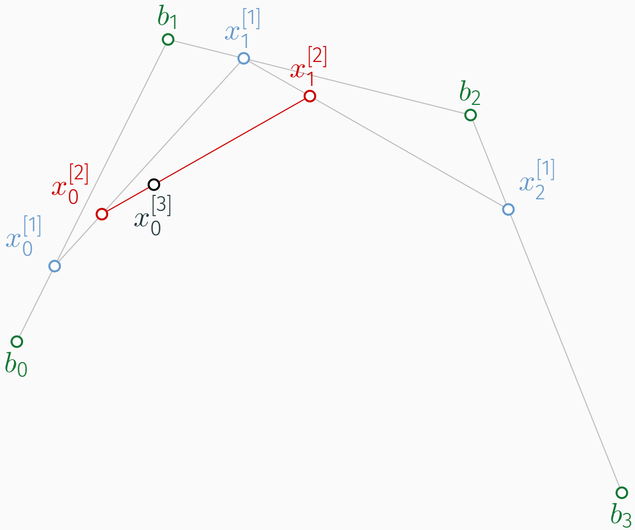

Repeat for the last segment to obtain $\beta_3(\frac{1}{4}; b_0, b_1, b_2, b_3) = x_0^{[3]}$.

Illustration of de Casteljau's Algorithm

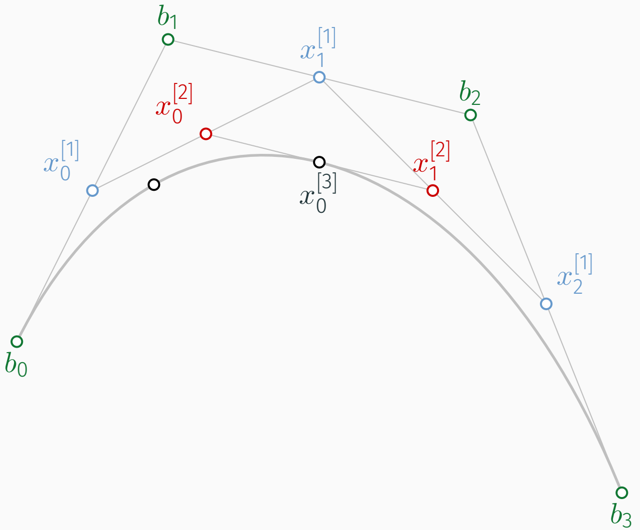

Same procedure for evaluation of $\beta_3(\frac{1}{2}; b_0, b_1, b_2, b_3)$.

Illustration of de Casteljau's Algorithm

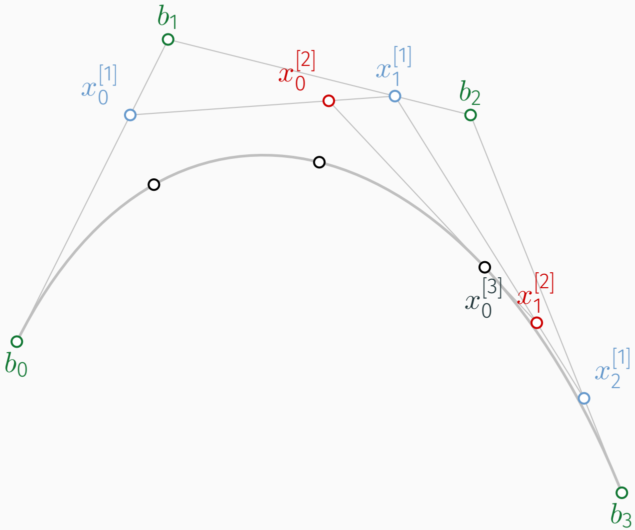

Same procedure for evaluation of $\beta_3(\frac{3}{4}; b_0, b_1, b_2, b_3)$.

Illustration of de Casteljau's Algorithm

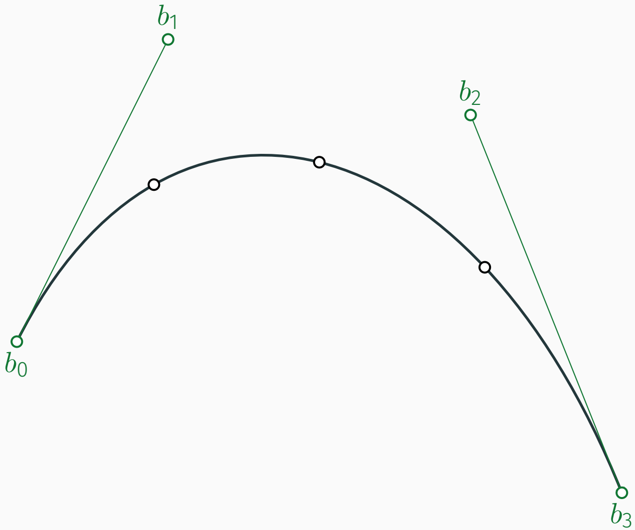

Complete curve $\beta_3(t; b_0, b_1, b_2, b_3)$.

Composite Bézier Curves

Definition
A composite Bezier curve $B\colon [0,n] \to \mathbb{R}^d$ is defined as

$$B(t) := \begin{cases} \beta_K(t; b_0^0, \ldots, b_K^0) & \text{if } t \in [0,1], \\ \beta_K(t-i; b_0^i, \ldots, b_K^i), & \text{if } t \in (i, i+1], \quad i = 1, \ldots, n-1. \end{cases}$$

Composite Bézier Curves

Definition
A composite Bezier curve $B\colon [0,n] \to \mathbb{R}^d$ is defined as

$$B(t) := \begin{cases} \beta_K(t; b_0^0, \ldots, b_K^0) & \text{if } t \in [0,1], \\ \beta_K(t-i; b_0^i, \ldots, b_K^i), & \text{if } t \in (i, i+1], \quad i = 1, \ldots, n-1. \end{cases}$$

Denote ith segment by $B_i(t) = \beta_K(t; b_0^i, \ldots, b_K^i)$ and $p_i = b_0^i$.

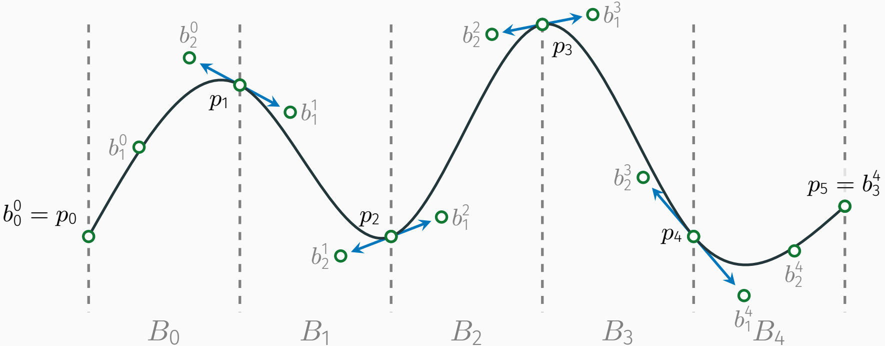

Composite Bézier Curves

Definition
A composite Bezier curve $B\colon [0,n] \to \mathbb{R}^d$ is defined as

$$B(t) := \begin{cases} \beta_K(t; b_0^0, \dots, b_K^0) & \text{if } t \in [0,1], \\ \beta_K(t-i; b_0^i, \dots, b_K^i), & \text{if } t \in (i, i+1], \quad i = 1, \dots, n-1. \end{cases}$$

Denote ith segment by $B_i(t) = \beta_K(t; b_0^i, \dots, b_K^i)$ and $p_i = b_0^i$.

- continuous iff $B_{i-1}(1) = B_i(0)$, $i = 1, \dots, n-1$
  $\Rightarrow b_K^{i-1} = b_0^i = p_i$, $i = 1, \dots, n-1$
- continuously differentiable iff $p_i = \frac{1}{2}(b_{K-1}^{i-1} + b_1^i)$

Bézier Curves on a Manifold

Definition. [Park, Ravani, 1995; Popiel, Noakes, 2007]
Let $\mathcal{M}$ be a Riemannian manifold and $b_0, \ldots, b_K \in \mathcal{M}$, $K \in \mathbb{N}$.

The (generalized) Bézier curve of degree k, $k \leq K$, is defined as

$$\beta_k(t; b_0, \ldots, b_k) = g(t; \beta_{k-1}(t; b_0, \ldots, b_{k-1}), \beta_{k-1}(t; b_1, \ldots, b_k)),$$

if $k > 0$, and

$$\beta_0(t; b_0) = b_0.$$

Definition. [Park, Ravani, 1995; Popiel, Noakes, 2007]
Let $\mathcal{M}$ be a Riemannian manifold and $b_0, \ldots, b_K \in \mathcal{M}$, $K \in \mathbb{N}$.

The (generalized) Bézier curve of degree k, $k \leq K$, is defined as

$$\beta_k(t; b_0, \ldots, b_k) = g(t; \beta_{k-1}(t; b_0, \ldots, b_{k-1}), \beta_{k-1}(t; b_1, \ldots, b_k)),$$

if $k > 0$, and

$$\beta_0(t; b_0) = b_0.$$

- Bézier curves $\beta_1(t; b_0, b_1) = g(t; b_0, b_1)$ are geodesics.
- composite Bézier curves $B\colon [0, n] \to \mathcal{M}$ completely analogue (using geodesics for line segments)

Bézier Curves on a Manifold

Definition. [Park, Ravani, 1995; Popiel, Noakes, 2007]
Let $\mathcal{M}$ be a Riemannian manifold and $b_0, \ldots, b_K \in \mathcal{M}$, $K \in \mathbb{N}$.

The (generalized) Bézier curve of degree k, $k \leq K$, is defined as

$$\beta_k(t; b_0, \ldots, b_k) = g(t; \beta_{k-1}(t; b_0, \ldots, b_{k-1}), \beta_{k-1}(t; b_1, \ldots, b_k)),$$

if $k > 0$, and

$$\beta_0(t; b_0) = b_0.$$

The Riemannian composite Bezier curve $B(t)$ is

- continuous iff $B_{i-1}(1) = B_i(0)$, $i = 1, \ldots, n-1$
  $\Rightarrow b_K^{i-1} = b_0^i =: p_i$, $i = 1, \ldots, n-1$
- continuously differentiable iff $p_i = g\left(\frac{1}{2}; b_{K-1}^{i-1}, b_1^i\right)$

Definition. [Park, Ravani, 1995; Popiel, Noakes, 2007]
Let $\mathcal{M}$ be a Riemannian manifold and $b_0, \ldots, b_K \in \mathcal{M}$, $K \in \mathbb{N}$.

The (generalized) Bézier curve of degree k, $k \leq K$, is defined as

$$\beta_k(t; b_0, \ldots, b_k) = g(t; \beta_{k-1}(t; b_0, \ldots, b_{k-1}), \beta_{k-1}(t; b_1, \ldots, b_k)),$$

if $k > 0$, and

$$\beta_0(t; b_0) = b_0.$$

The Riemannian composite Bezier curve $B(t)$ is

- continuous iff $B_{i-1}(1) = B_i(0)$, $i = 1, \ldots, n-1$
  $\Rightarrow b_K^{i-1} = b_0^i =: p_i$, $i = 1, \ldots, n-1$
- continuously differentiable iff $b_{K-1}^{i-1} = g\big(2; b_1^i, p_i\big)$.

Illustration of a Composite Bézier Curve on the Sphere $\mathbb{S}^2$

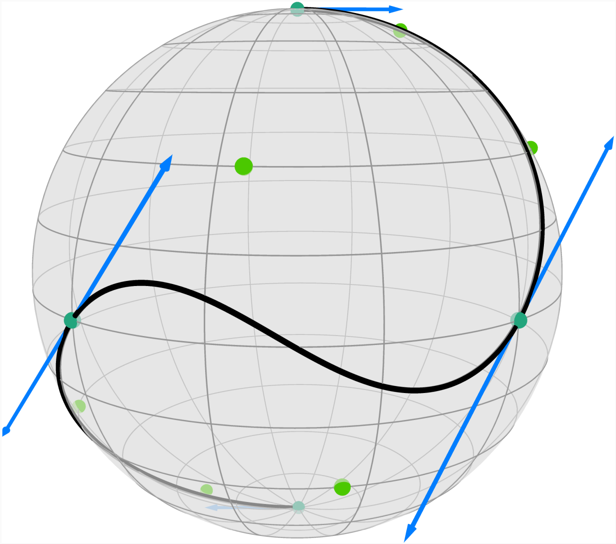

The directions, e.g. $\log_{p_j} b_j^1$, are now tangent vectors.

A Variational Model for Data Fitting

Let $d_0, \ldots, d_n \in \mathcal{M}$. A model for data fitting reads

$$\mathcal{E}(B) = \frac{\lambda}{2} \sum_{k=0}^{n} d^2_{\mathcal{M}}(B(k), d_k) + \int_0^n \Bigl\lVert \frac{D^2 B(t)}{\mathrm{d}t^2} \Bigr\rVert^2_{B(t)} \mathrm{d}t, \qquad \lambda > 0,$$

where $B \in \Gamma$ is from the set of continuously differentiable composite Bezier curve of degree K with n segments.

A Variational Model for Data Fitting

Let $d_0, \ldots, d_n \in \mathcal{M}$. A model for data fitting reads

$$\mathcal{E}(B) = \frac{\lambda}{2} \sum_{k=0}^{n} d^2_{\mathcal{M}}(B(k), d_k) + \int_0^n \left\| \frac{D^2 B(t)}{\mathrm{d}t^2} \right\|^2_{B(t)} \mathrm{d}t, \qquad \lambda > 0,$$

where $B \in \Gamma$ is from the set of continuously differentiable composite Bezier curve of degree K with n segments.

- Goal: find minimizer $B^* \in \Gamma$
- finite dimensional optimization problem in the control points b^i_j, i.e. on $\mathcal{M}^L$ with
  - $L = n(K-1) + 2$
  - $\lambda \to \infty$ yields interpolation $(p_k = d_k) \Rightarrow L = n(K-2) + 1$

A Variational Model for Data Fitting

Let $d_0, \ldots, d_n \in \mathcal{M}$. A model for data fitting reads

$$\mathcal{E}(B) = \frac{\lambda}{2}\sum_{k=0}^{n} d^2_{\mathcal{M}}(B(k), d_k) + \int_0^n \Bigl\| \frac{D^2 B(t)}{\mathrm{d}t^2} \Bigr\|^2_{B(t)} \mathrm{d}t, \qquad \lambda > 0,$$

where $B \in \Gamma$ is from the set of continuously differentiable composite Bezier curve of degree K with n segments.

- Goal: find minimizer $B^* \in \Gamma$
- finite dimensional optimization problem in the control points b^i_j, i.e. on $\mathcal{M}^L$ with
  - $L = n(K-1) + 2$
  - $\lambda \to \infty$ yields interpolation $(p_k = d_k) \Rightarrow L = n(K-2) + 1$
- On $\mathcal{M} = \mathbb{R}^m$: closed form solution, natural (cubic) splines

Discretizing the Data Fitting Model

We discretize the absolute second order covariant derivative

$$\int_0^n \left\| \frac{D^2 B(t)}{\mathrm{d}t^2} \right\|_{\gamma(t)}^2 \mathrm{d}t \approx \sum_{k=1}^{N-1} \frac{\Delta_s d_2^2[B(s_{i-1}), B(s_i), B(s_{i+1})]}{\Delta_s^4}.$$

on equidistant points $s_0, \ldots, s_N$ with step size $\Delta_s = s_1 - s_0$.

Evaluating $\mathcal{E}(B)$ consists of evaluation of geodesics and squared (Riemannian) distances

- $(N+1)K$ geodesics to evaluate the Bézier segments
- N geodesics to evaluate the mid points
- N squared distances to obtain the second order absolute finite differences squared

Gradient of the Discretized Data Fitting Model

For the gradient of the discretized data fitting model

$$\mathcal{E}(B) = \frac{\lambda}{2}\sum_{k=0}^{n} d^2_{\mathcal{M}}(B(k), d_k) + \sum_{k=1}^{N-1} \frac{\Delta_s d_2^2[B(s_{i-1}), B(s_i), B(s_{i+1})]}{\Delta_s^4}.$$

we

- identified first and last control points $p_i = b_K^{i-1} = b_0^i$
- plug in the constraint $b_{K-1}^{i-1} = g(2; b_1^i, p_i)$
  $\Rightarrow$ Introduces a further chain rule for the differential
  $\Rightarrow$ reduces the number of optimization variables.
- concatenation of adjoint Jacobi fields (evaluated at the points s_i) yields the gradient $\nabla_{\mathcal{N}}\mathcal{E}$.

Gradient Descent on a Manifold

Let $\mathcal{N} = \mathcal{M}^L$ be the product manifold of $\mathcal{M}$,

Input.

- $\mathcal{E} \colon \mathcal{N} \to \mathbb{R}$,
- its gradient $\nabla_{\mathcal{N}}\mathcal{E}$,
- initial data $q^{(0)} = b \in \mathcal{N}$
- step sizes $s_k > 0, k \in \mathbb{N}$.

Output: $\hat{q} \in \mathcal{N}$

$k \leftarrow 0$

repeat

$\quad q^{(k+1)} \leftarrow \exp_{q^{(k)}}\bigl(-s_k \nabla_{\mathcal{N}}\mathcal{E}(q^{(k)})\bigr)$

$\quad k \leftarrow k+1$

until a stopping criterion is reached

return $\hat{q} \coloneqq q^{(k)}$

Armijo Step Size Rule

Let $q = q^{(k)}$ be an iterate from the gradient descent algorithm, $\beta, \sigma \in (0, 1), \alpha > 0$.

Let m be the smallest positive integer such that

$$\mathcal{E}(q) - \mathcal{E}\big(\exp_q(-\beta^m \alpha \nabla_{\mathcal{N}} \mathcal{E}(q))\big) \geq \sigma \beta^m \alpha \|\nabla_{\mathcal{N}} \mathcal{E}(q)\|_q$$

holds. Set the step size $s_k \coloneqq \beta^m \alpha$.

Minimizing with Known Minimizer

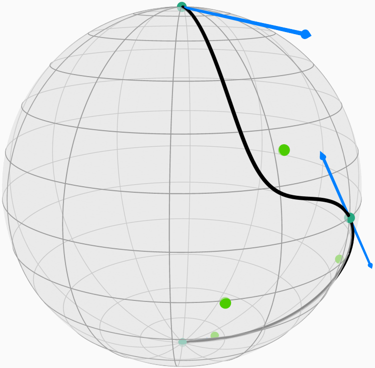

Original

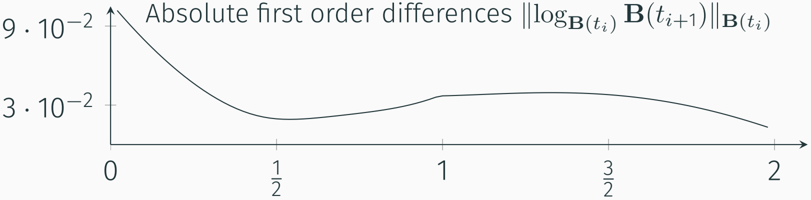

Minimizing with Known Minimizer

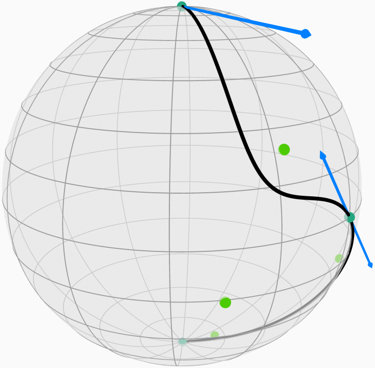

Original

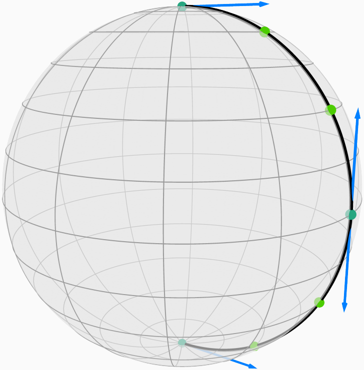

Minimized

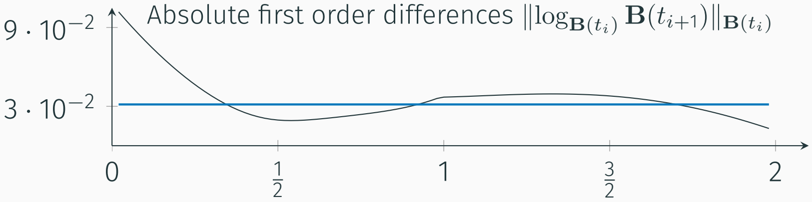

Interpolation by Bézier Curves with Minimal Acceleration.

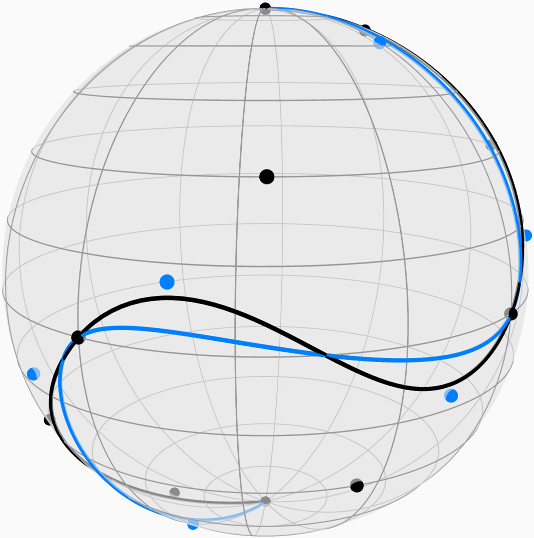

A comp. Bezier curve (black) and its mnimizer (blue).

Approximation by Bézier Curves with Minimal Acceleration.

In the following video λ is slowly decreased from 10 to 0.

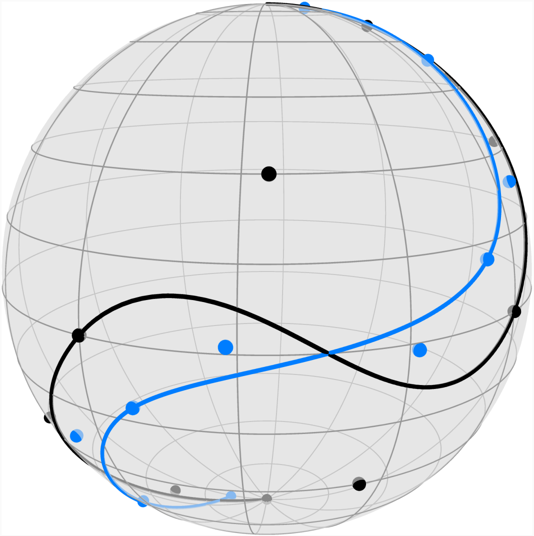

The initial setting, $\lambda = 10$.

Approximation by Bézier Curves with Minimal Acceleration.

In the following video λ is slowly decreased from 10 to 0.

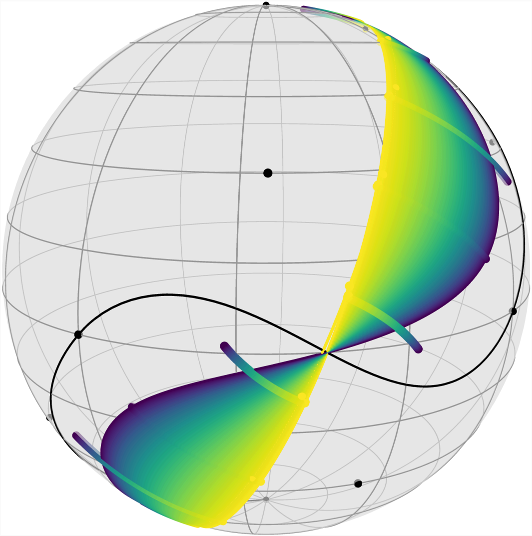

Summary of reducing λ from 10 (violet) to zero (yellow).

Comparison to Previous Approach

[Gousenbourger, Massart, Absil, 2018]

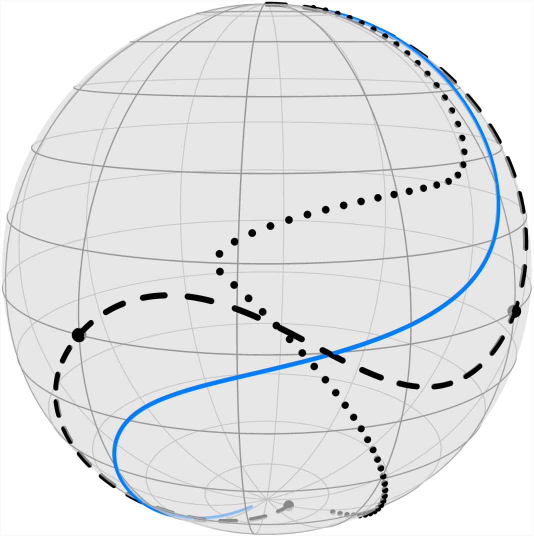

This curve (dashed) is “too global” to be solved in a tangent space (dotted) correctly, while our method (blue) still works.

An Example of Rotations $\mathcal{M} = \mathrm{SO}(3)$

Initialization with approach from composite splines

[Gousenbourger, Massart, Absil, 2018]

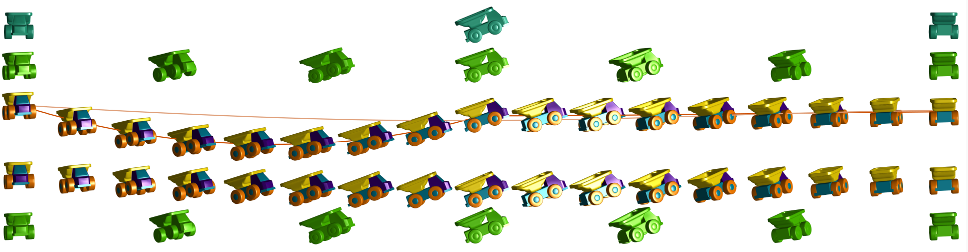

Our method outperforms the approach of solving linear systems in tangent spaces, but their approach can serve as an initialization.

Further Models and Algorithms

Models in manifold-valued imaging.

- Infimal Convolution [Bergmann, Fitschen, et al., 2017 ; Bergmann, Fitschen, et al., 2018]
- TGV [Bergmann, Fitschen, et al., 2018; Bredies et al., 2018]
- Nonlocal TV using the Graph Laplacian [Bergmann, Tenbrinck, 2018]
- denoising using second order statistics [Laus et al., 2017]

Algorithms In manifold-valued imaging.

- Douglas–Rachford splitting on Hadamard manifolds [Bergmann, Persch, Steidl, 2016]
- Half-quadratic Minimization (iteratively reweighted least squares) [Bergmann, Chan, et al., 2016; Grohs, Sprecher, 2016]

Summary

We defined second order differences on Riemannian manifolds.

Two variational models: second order total variation and minimizing the acceleration of a Bézier curve.

We further presented two algorithms to minimize the corresponding Variational Models: Cyclic Proximal Point Algorithm (for nonsmooth) and Gradient Descent (for smooth) to minimize the model.

Future Work

- further models (Bézier surfaces, manifolds with no closed form for Jacobi fields,…)
- further algorithms, e.g. for constraint optimization
- further manifolds, e.g. infinite dimensional ones

Implement Algorithms in `Manopt.jl` an upcoming manifold optimization toolbox for Julia paradigm:

Being able to use an(y) algorithm for a(ny) model directly on a(ny) manifold efficiently.

…in an open source programming language.

Selected References on Total Variation

Bačák, M.; Bergmann, R.; Steidl, G.; Weinmann, A. (2016). “A Second Order Non-Smooth Variational Model for Restoring Manifold-Valued Images”. *SIAM Journal on Scientific Computing* 38.1, A567–A597. DOI: 10.1137/15M101988X.

Bergmann, R.; Fitschen, J. H.; Persch, J.; Steidl, G. (2018). “Priors with Coupled First and Second Order Differences for Manifold-Valued Image Processing”. *Journal of Mathematical Imaging and Vision* 60.9, pp. 1459–1481. DOI: 10.1007/s10851-018-0840-y.

Bergmann, R.; Tenbrinck, D. (2018). “A graph framework for manifold-valued data”. *SIAM Journal on Imaging Sciences* 11.1, pp. 325–360. DOI: 10.1137/17M1118567.

Laus, F.; Nikolova, M.; Persch, J.; Steidl, G. (2017). “A Nonlocal Denoising Algorithm for Manifold-Valued Images Using Second Order Statistics”. *SIAM Journal on Imaging Sciences* 10.1, pp. 416–448. DOI: 10.1137/16M1087114.

Lellmann, J.; Strekalovskiy, E.; Koetter, S.; Cremers, D. (2013). “Total variation regularization for functions with values in a manifold”. *IEEE ICCV 2013*, pp. 2944–2951. DOI: 10.1109/ICCV.2013.366.

Weinmann, A.; Demaret, L.; Storath, M. (2014). “Total variation regularization for manifold-valued data”. *SIAM Journal on Imaging Sciences* 7.4, pp. 2226–2257. DOI: 10.1137/130951075.

Selected References on Bézier Curves

Arnould, A.; Gousenbourger, P.-Y.; Samir, C.; Absil, P.-A.; Canis, M. (2015). "Fitting Smooth Paths on Riemannian Manifolds : Endometrial Surface Reconstruction and Preoperative MRI-Based Navigation". *GSI2015*. Ed. by F.Nielsen; F.Barbaresco. Springer International Publishing, pp. 491–498. DOI: 10.1007/978-3-319-25040-3_53.

Bergmann, R.; Gousenbourger, P.-Y. (2018). "A variational model for data fitting on manifolds by minimizing the acceleration of a Bézier curve". *Frontiers in Applied Mathematics and Statistics*. DOI: 10.3389/fams.2018.00059. arXiv: 1807.10090.

Boumal, N.; Absil, P. A. (2011). "A discrete regression method on manifolds and its application to data on SO(n)". *IFAC Proceedings Volumes (IFAC-PapersOnline)*. Vol. 18. PART 1, pp. 2284–2289. DOI: 10.3182/20110828-6-IT-1002.00542.

Gousenbourger, P.-Y.; Massart, E.; Absil, P.-A. (2018). "Data fitting on manifolds with composite Bézier-like curves and blended cubic splines". *Journal of Mathematical Imaging and Vision*. accepted. DOI: 10.1007/s10851-018-0865-2.

Samir, C.; Absil, P.-A.; Srivastava, A.; Klassen, E. (2012). "A Gradient-Descent Method for Curve Fitting on Riemannian Manifolds". *Foundations of Computational Mathematics* 12.1, pp. 49–73. DOI: 10.1007/s10208-011-9091-7.